Research Article

Journal of Applied Toxicology

Received: 29 January 2013, Revised: 22 March 2013, Accepted: 23 March 2013 Published online in Wiley Online Library: 24 May 2013

(wileyonlinelibrary.com) DOI 10.1002/jat.2887

Toxicity assessment of manganese oxide micro and nanoparticles in Wistar rats after 28 days of repeated oral exposure

Shailendra Pratap Singh, Monika Kumari, Srinivas I. Kumari, Mohammed F. Rahman, M. Mahboob and Paramjit Grover*

ABSTRACT: In the near future, nanotechnology is envisaged for large-scale use. Hence health and safety issues of nanoparticles (NPs) should be promptly addressed. Twenty-eight-day oral toxicity, genotoxicity, biochemical alterations, histopathological changes and tissue distribution of nano and microparticles (MPs) of manganese oxide (MnO_2) in Wistar rats was studied. Genotoxicity was assessed using comet, micronucleus and chromosomal aberration assays. The results demonstrated a significant increase in DNA damage in leukocytes, micronuclei and chromosomal aberrations in bone marrow cells after exposure of MnO_2-NPs at 1000, 300 mg kg^{-1} bw per day and MnO_2-MPs at the dose of 1000 mg kg^{-1} bw per day. Our findings showed acetylcholinestrase inhibition at 1000 as well as at 300 mg kg^{-1} bw per day in blood and with all the doses in the brain indicating the toxicity of MnO_2-NPs. Further, the doses significantly inhibited different ATPases in the brain P_2 fraction. Significant changes were observed in aspartate aminotransferase (AST), alanine aminotransferase (ALT) and lactate dehydrogenase (LDH) in the liver, kidney and serum in a dose-dependent manner. MnO_2-MPs at 1000 mg kg^{-1} bw per day were found to induce significant alterations in biochemical enzymes. A significant distribution was found in all the tissues in a dose-dependent manner. MnO_2-NPs showed a much higher absorptivity and tissue distribution as compared with MnO_2-MPs. A large fraction of MnO_2-NPs and MnO_2-MPs was cleared by urine and feces. Histopathological analysis revealed that MnO_2-NPs caused alterations in liver, spleen, kidney and brain. The MnO_2-NPs induced toxicity at lower doses compared with MnO_2-MPs. Further, this study did not display gender differences after exposure to MnO_2-NPs and MnO_2-MPs. Therefore, the results suggested that prolonged exposure to MnO_2 has the potential to cause genetic damage, biochemical alterations and histological changes. Copyright © 2013 John Wiley & Sons, Ltd.

Keywords: MnO_2-NPs; MnO_2-MPs; genotoxicity; biochemical parameters; biodistribution; Wistar rats

Introduction

Nanotechnology involves the production of materials at the nanoscale to manufacture novel products with unique properties. Nanoscience has attracted extensive investment worldwide owing to several uses of engineered nanoparticles (NPs). Hence, nanotechnology is being projected as a trillion dollar industry by 2015 (Nel *et al*., 2006). NPs can be defined as materials having a single dimensional feature within 1–100 nm range. The unique properties of NMs have increased concerns with regards to toxic effects on humans and the environment. Commercialization of nanomaterials is rapidly overtaking efforts to study their impact on human and environment health (Service, 2005). Toxicological studies are therefore necessary to find out the likely adverse effects of NPs.

Manganese oxide (MnO_2)-NPs are promising materials used as contrast agents for magnetic resonance imaging (MRI), drug delivery, an ionization-assisting reagent in mass spectroscopy, waste water treatment and consumer products such as batteries (Chen andHe, 2008; Na *et al*., 2007; Rutz, 2009; Shin *et al*., 2009; Taira *et al*., 2009). The increase in the production and use of Mn oxide NPs may enhance the probable risk to occupationally exposed humans and the environment. Most of the toxicity investigations reported with Mn oxide NPs are either *in vitro* or *in vivo* studies on the respiratory system. Toxicity evaluation using a variety of *in vitro* assays was carried out in BRL 3A rat liver cells using different NPs including MnO_2. Results showed that MnO_2-NPs displayed lactate dehydrogenase (LDH) leakage only at higher doses (100–250 μg ml^{-1}) (Hussain *et al*., 2005). The neuroendocrine cell line (PC-12) was exposed to MnO_2-NPs, cellular morphology, mitochondrial function and dopamine was assessed after 24 h. Mitochondrial reduction activity and metal cytotoxicity showed moderate toxicity for Mn-40 nm. Further, Mn-40 nm induced dose-dependent dopamine depletion (Hussain *et al*., 2006). Human lung epithelial cells (A549) when exposed to Mn_3O_4-NPs showed reactive oxygen species (ROS) formation (Limbach *et al*., 2007). The neurotoxicity of Mn oxide NPs of different sizes and compositions was investigated using ST14 rat striated neuroblasts. The results revealed that induction of oxidative stress and cell death took place via apoptosis (Stefanescu *et al*., 2009). Lung adenocarcinoma, breast cancer cells and glioblastoma cells exposed to MnO_2-NPs using the live/dead cell assay, LDH assay and reactive oxygen species (ROS) detection showed cytotoxicity (Choi *et al*., 2010). N27 dopaminergic neuronal cells exposed to nanosized Mn

*Correspondence to: Paramjit Grover, Toxicology Unit, Biology Division, Indian Institute of Chemical Technology, Hyderabad – 500 007, Andhra Pradesh, India. E-mail: paramgrover@gmail.com or grover@iict.res.in

Toxicology Unit, Biology Division, Indian Institute of Chemical Technology, Hyderabad, 500 007, Andhra Pradesh, India

at 25–400 μg ml^{-1} activated mitochondrial-dependent apoptotic signaling and autophagy in a time and dose-dependent manner (Nagwa *et al.*, 2011). Rat type II alveolar epithelial cells exposed to MnO_2-NPs generated oxidative stress, cellular uptake and apoptosis (Frick *et al.*, 2011). MnO_2 exposed to rats using a subacute intratracheal method showed a decrease in body weight. The relative weight of lungs increased and that of the liver decreased in a dose- and time-dependent manner in the NMs-exposed animals. Mn was detected in their lung and brain tissues indicating that the instilled NMs had crossed from the airways to the brain (Sarkozi *et al.*, 2009). Subchronic exposure of MnO_2-NPs to rats by intra-nasal and intra-tracheal routes, showed a significant increase in Mn levels in the brain and blood as well as functional alterations (Oszlanczi *et al.*, 2010a, 2010b).

However, as far as we are aware repeated dose oral toxicity of MnO_2-NPs in rats has not been investigated to date. *In vivo* study of NPs is essential because animal systems are extremely complicated and the interaction of the NPs with biological systems could lead to novel biodistribution, clearance, immune response and metabolism patterns (Fischer and Chan, 2007). Moreover, the gastrointestinal tract is an important portal of entry of NPs in humans and animals.

Hence, we have conducted a 28-day repeated oral dose toxicity study of MnO_2-NPs and microparticles (MPs) in albino Wistar male and female rats.

The characterization of NPs is mandatory in order to understand the potential toxicity to biological components (Murdock *et al.*, 2008). Hence in the present study, the physicochemical properties of MnO_2-NPs and MnO_2-MPs were measured. Worries of the hazards of mutation and cancer induction are worldwide and as a result genotoxicity studies are an important part of safety assessment of chemicals. The *in vivo* genotoxicity of MnO_2-NPs and MnO_2-MPs was studied using comet assay (Tice *et al.*, 2000), micronucleus test (MNT) (Schmid, 1975) and chromosomal aberration (CA) assay (Adler, 1984). Biochemical parameters such as acetylcholinesterase (AChE), different ATPases (Na^+-K^+-, Mg^{2+} and Ca^{2+}-ATPase), alanine aminotransferase (ALT), aspartate minotransferase (AST) and the LDH assay were evaluated in various organs of the treated rats. Histological studies are a reliable method to detect morphological changes owing to toxicants; hence histopathology of various treated tissues was carried out. Biodistribution study of NPs is essential to understand the amount of NPs that enter in the target tissue or site and whether translocated across the body surface. It is important to know their anatomic fate, clearance and biological effects.

In the present investigation, a 28-day repeated oral dose study of MnO_2-NPs and MnO_2-MPs was carried in albino Wistar male and female rats. The effect of the particles on the body weight and feed intake was examined. Genotoxicity assays such as the comet assay in peripheral blood, MNT and CA in bone marrow cells were performed. Target biochemical parameters namely AChE, different ATPases, ALT, AST and LDH were assessed in serum, blood and various tissues such as the liver, kidney and brain. Histopathological examination of the liver, kidney, spleen, heart and brain was carried out from treated and control rats. Moreover, the effect of the test compounds on biodistribution in rat's whole blood, liver, kidney, heart, brain, spleen, lungs, urine and feces was analyzed using inductively coupled plasma-mass spectrophometery (ICP-MS).

Materials and Methods

Chemicals

MnO_2 nanoparticles of size < 30 nm and purity $\geq 98.1\%$ (according to the manufacture's report) were purchased from Mukherjee Industries Kolkata, India. MnO_2-MPs of size < 5 μm and purity $\geq 99\%$ (CAS No. 1313-13-9), low-melting point agarose (LMA), normal-melting point agarose (NMA), ethyline-diaminotetraacetic acid (EDTA) disodium salt, phosphate-buffered saline (Ca^{2+}, Mg^{2+} free; PBS), Ouabain, Ethylene Glycol bis-(amino ethyl ether) tetra acetic acid (EGTA), Giemsa stain and Quinidine sulphate were purchased from Sigma Chemical Co., St Louis, USA. Adenosine triphosphate (ATP) and Tris hydrochloride were obtained from Hi-Media, Mumbai, India. Cyclophosphamide (CP), purchased from Endoxan Asta, Asta Medica A.G., Frankfurt,, Germany was dissolved in distilled water just before use.

Characterization of Particles

The primary size of the particles was estimated by transmission electron microscopy (TEM) and images of MnO_2-NPs and its MnO_2-MPs were taken to obtain size and morphology on a TEM (JEM-2100) from JEOL Ltd., Tachikawa, Tokyo, Japan at an accelerating voltage of 120 kV. The particles were examined using Advanced Microscopy Techniques (AMT) software for the digital TEM camera calibrated for size measurement. One hundred particles were calculated from random fields of view in addition to images that show general morphology of the particles.

The particle size distribution of the NPs and agglomerates in solution were measured by dynamic light scattering (DLS) and laser Doppler velocimetry (LDV) using a Malvern Instruments Zetasizer Nano-ZS Instrument. The device uses a 4 mW He-Ne 633 nm laser to analyze the samples as well as an electric field generator for laser Doppler velocimetry measurements. Fifty ppm of freshly prepared MnO_2-NPs suspension in Milli Q water was sonicated using a probe sonicator (UPH 100; Hielscher Ultrasonics GmbH, Teltow, Germany) for 10 min. The prepared samples were transferred to a 1.5-ml square cuvette for DLS measurements and 1 ml was transferred to a Malvern Clear Zeta Potential cell for LDV measurement. The mean NPs diameter was calculated by the software and the polydispersity index (PdI) given was a measure of the size ranges present in the solution. The PdI scale ranges from 0 to 1, with 0 being monodisperse and 1 being polydisperse.

The specific surface areas ($m^2 g^{-1}$) of the MnO_2-NPs and MnO_2-MPs were measured by N_2 adsorption–desorption measurement at 77 K by the Brunauer–Emmett–Teller (BET) method using a surface area analyzer Quadrusorb-SI V 5.06 instrument (M/S Quanta chrome Instruments Corporation, Boynton Beach, FL, USA).

Animals

Albino Wistar male and female rats aged 6–8 weeks and weighing 80–120 g were obtained from National Institute of Nutrition, Hyderabad, India. The rats were housed for a week for acclimatization in groups of five in standard polypropylene cages with a stainless steel top grill. Clean paddy husk was used as a bedding material. The animals were fed a commercial pellet diet and water *ad libitum* in polypropylene bottles with stainless

steel sipper tubes. The animals were maintained under standard conditions of humidity (55–65%), temperature (22±3 °C) and light (12-h light/12-h dark cycles). The study was approved by Institutional Animal Ethical Committee of our institute, India.

Treatment of Animals

MnO_2-NPs and MnO_2-MPs were suspended in MilliQ water, properly ultrasonicated (UP100H; Hielscher Ultrasonics GmbH, Teltow, Germany) and vortexed before every treatment of the rats. A 28-day repeated dose oral toxicity study was conducted with male and female rats by dividing them into four groups (10 rats; 5 males and 5 females in each group): control, low dose (30 mg kg^{-1} bw per day), medium dose (300 mg kg^{-1} bw per day) and high dose (1000 mg kg^{-1} bw per day) of MnO_2-NPs and MnO_2-MPs treated using the oral route daily for 28 days using a suitable intubation cannula. The highest dose was selected based on induction of a toxic effect without severe sufferings and mortality, whereas the lowest dose demonstrated slight adverse effects. Rats were exposed daily for 28 days by oral gavage and all the treated rats were sacrificed by cervical dislocation after 24 h of last administration of a dose. Cyclophosphamide, a known mutagen, was used as the positive control for genotoxicity studies at a dose 40 mg kg^{-1} bw and the volume injected was 0.01 ml g^{-1} bw. This was given intraperitonially (i.p.) 24 h before sacrifice.

Comet Assay (Single Cell gel Electrophoresis)

To investigate the *in vivo* genotoxicity effects of the MnO_2-NPs and MnO_2-MPs after 28-day repeated oral dosing in male and female Wistar rats at various doses (30, 300, 1000 mg kg^{-1} bw per day), a single-cell gel electrophoresis analysis (comet assay) was used. The alkaline comet assay was conducted for the assessment of DNA damage according to the guidelines proposed by Tice *et al*. (2000) with slight modifications. Three slides were prepared for each experimental point. Cell viability was determined by the trypan blue exclusion assay (Pool-Zobel *et al*., 1994). Peripheral blood was collected at the 28th day from male and female rats. One hundred cells per rat (50 cells analysed in each slide) were scored at 400× using a fluorescence microscope (Olympus Corporation, Shinjuku-ku, Tokyo, Japan) with a blue (488 nm) excitation filter and yellow (515 nm) emission (barrier) filter. One scorer analyzed the slides throughout the study and all the slides were coded. Detection of DNA breakage was measured using a Comet Image Analysis System, version 6 (Kinetic Imaging Ltd, Nottingham, UK). The % tail DNA damage was used to evaluate DNA damage.

Micronucleus Test

For the MN analysis, the method described by Schmid (1975) was used in the bone marrow cells, which were extracted from thigh bone of rats. The male and female rats were sacrificed 24 h after the last administration. The femurs were removed, the bone marrow collected, centrifuged, spread on the slides and allowed to dry in humidified air overnight. The slides were fixed with methanol and stained with Giemsa, prepared in PBS, for the assessment of the micronuclei (MN) occurrence. The study was done according to OECD Guideline 474 (OECD 1997a). Three slides were made for each animal; the slides were microscopically analyzed at 1000× magnification. Per animal, 2000 PCEs were randomly selected from three slides and scored for the presence of MN.

Chromosomal Aberration Assay

CA analysis was done by the method of rinsing the rat's bone marrow cells (femur and tibia) as described by Adler (1984) after 28-day repeated oral treatment with the various doses (30, 300, 1000 mg kg^{-1} bw per day) of MnO_2-NPs and MnO_2-MPs in male and female Wistar rats. The analysis was carried out at 28th day. The bone marrow was collected and centrifuged. Cells were then fixed through several changes of ice-cold methanol/glacial acetic acid (3:1, v/v) until the pellets were clean. After refrigeration for at least 24 h, cells were centrifuged and resuspended in fresh fixative, dropped onto slides, dried and stained with Geimsa. Three slides for each animal were made by the flame-dried technique. CAs were identified on the basis of criteria established by the OECD Guideline 475 (OECD 1997b). Five hundred well spread metaphases were selected to detect the presence of CAs. The mitotic index (MI) was determined with 1000 or more cells.

Biochemical Assays

Serum was collected by centrifuging blood without any anticoagulant at 176 g for 10 min. Different tissues such as the liver, kidney and brain of both control and treated rats were dissected and quickly homogenized separately in ice-cold 0.25 M sucrose using a Miccra D-1-high speed tissue homogenizer to make 10% homogenate (w/v). The homogenate was centrifuged at 10 000 *g* for 10 min at 4 °C. The pellet was discarded and the supernatant was used as enzyme source. Serum and supernatant of the homogenate of liver and kidney were used to determine the AST and ALT according to the method of Yatzidis (1960) and LDH by the method of McQueen (1972). Red blood cells (RBC) and brain AChE was determined according to the method of Ellman *et al*. (1961).

Estimation of Different ATPases in Brain P_2 Fractionation

The homogenization and subsequent fractionation of brain for different ATPases were done according to the method described by Jinna *et al*. (1989). Centrifugation of the post nuclear fraction at 13 000 *g* for 20 min resulted in the P_2 fraction, which consisted of nerve endings and mitochondria and was used for the assay of various ATPases. The inorganic phosphate liberated was estimated by the method of Fiske and Subbarow (1925). Protein was determined as described by Lowry *et al*. (1951).

Histopathology

Histopathology of the liver, kidney, spleen, heart and brain was carried out in control and treated animals after 28-day repeated oral dose. After sacrifice, tissues were washed with 1% ice cold saline and fixed in neutral buffered 10% formalin. The tissues were embedded in paraffin blocks, then trimmed and sectioned using a microtome. Paraffin sections of 3 μm thickness were stained with hematoxylin & eosin and mounted on a glass microscope slide. The slides were examined with Nikon Eclipse E 800 microscope at 400 ×.

Mn Content Analysis in Tissues

A biodistribution study of the MnO_2-NPs and MnO_2-MPs in the male and female Wistar rats was carried out after 28 days of repeated oral treatment. The animals were dosed with 30, 300, 1000 mg kg^{-1} bw per day of MnO_2-NPs and MnO_2-MPs and placed in metabolic cages to collect the urine and feces samples. Whole blood, liver, kidneys, heart, brain, spleen and lungs were taken out after sacrifice of rats at the 28th day. Prior to elemental analysis, approximately ~ 0.3 g of fresh liver, kidneys, heart, brain, spleen, feces and ~ 0. 3 ml of blood and urine samples were taken from all the treated rats. They were pre-digested in nitric acid overnight. The samples were then heated at 80 °C for 10 h followed by additional heating at 130–150 °C for 30 min. Finally, in the presence of 0.5 ml of 70% perchloric acid, the samples were again heated for 4 h and evaporated nearly to dryness. After digestion, the samples were filtered and made up to 25 ml using milli Q water for analysis. The Mn content in the samples after the 28-day repeated oral dose study in male and female wistar rats was determined by ICP-MS.

Statistical Analysis

The statistical significant changes were analyzed by one-way ANOVA. Results were expressed as mean±standard deviation (SD). Multiple comparisons were performed using the Dunnett test. All calculations were performed using Graph Pad Instat 3 Software package for windows (GraphPad Software, Inc., La Jolla, CA, USA). The statistical significance for all tests was set at $P < 0.05$.

Results

Characteristics of MnO_2 Nano and Micro Particles

The physico-chemical characteristics of MnO_2 particles were determined by TEM, DLS, LDV and BET analysis. The data obtained are shown in Table 1. The primary particle size and appearance of the MnO_2-NPs and MPs was determined by TEM images (Fig. 1A,B). The shape of particles was found to be spherical. The observed average mean size diameter of MnO_2-NPs and MnO_2-MPs was 42.63±23 nm and 2.95±31 μm, respectively. The DLS value for MnO_2 NPs size in the Milli Q water suspension was 324.8 nm. The result of DLS showed larger values than NPs size measured by TEM, indicating that MnO_2-NPs formed larger agglomerates in water suspension. Zeta potential and electrophoretic mobility measurements were −1.27 mV and 4.43 μ (μm·cm/V/s), respectively, at pH 7.0. DLS and LDV data were found to be out of the detection limit, in the case of MPs material. The specific surface area of MnO_2-NPs and MnO_2-MPs determined by BET analysis was 52.21 and 7.24 ($m^2 g^{-1}$) respectively.

Animal Observation, Food Consumption, Body Weight and Organ Weight

No adverse sign, symptoms and mortality were observed after 28-day repeated oral doses of 30, 300, 1000 mg kg^{-1} bw per day of MnO_2-NPs and MnO_2-MPs in male and female Wistar rats. However, MnO_2-NPs at high, medium and MnO_2-MPs at higher dose treated rats showed dullness, irritation and moribund

Table 1. Particle characterization of manganese oxide nanoparticles (MnO_2-NPs) and MnO_2-microparticles (MPs)

Particles	Size using TEM	DLS			LDV		Surface area ($m^2 g^{-1}$)
		Average diameter (nms)	PDI	Zeta potential ζ (mV)	Electrophoretic mobility μ (μm·cm/V/s)	pH	
MnO_2NPs	42·63±23(nm)	324·8	0·539	−1·27	4·43	7·0	52·21
MnO_2MPs	2·95±31(μm)	-	-	-	-	7·0	7·24

MnO_2-NPs and MnO_2-MPs were dispersed in MilliQ water and mixing was done via probe sonication for 10 min.
TEM, transmission electron microscopy; DLS, dynamic light scattering; LDV, laser Doppler velocimetry.

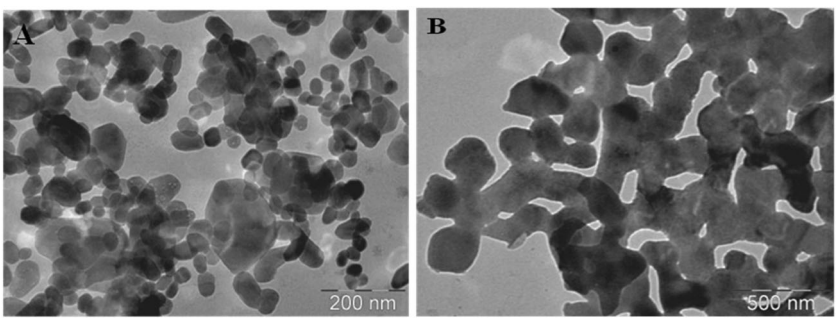

Figure 1. Transmission electron microscopy (TEM) images of manganese oxide nanoparticles (MnO_2-NPs) (A) and MnO_2-microparticles (MPs) (B). MnO_2-NPs and MnO_2-MPs were dispersed in MilliQ water, mixing was done via probe sonication for 10 min.

symptoms. However, mortality was not observed in this group of animals. Further, both nano and micro particles treated rats showed a reduction in body weight gain and feed intake (data not shown), but the loss was not significant. The percentage body weight decrease was in the range of 4.2–8.9% in the MnO_2-NPs-treated groups and 2.5–6.7% in the MnO_2-MPs-treated groups.

Comet Assay

The comet assay results after a 28-day repeated oral treatment with 30, 300, 1000 mg kg^{-1} bw per day of MnO_2-NPs and MnO_2-MPs in male and female Wistar rats are shown in Fig. 2A. In all samples, the cell viability by the trypan blue exclusion technique was > 90% (data not shown). A statistically significant ($P < 0.01$) increase in the DNA damage (% tail DNA) was observed in the peripheral blood leucocytes (PBL) of rats exposed to MnO_2-NPs with the highest and medium doses (1000 and 300 mg kg^{-1} bw per day) in both male and female rats. However, no significant DNA damage was observed with 30 mg kg^{-1} bw per day. A significant increase in % tail DNA was observed only with the higher dose (1000 mg kg^{-1} bw per day) in the MnO_2-MP-treated groups in both male and female rats. In rats treated orally with 300 and 30 mg kg^{-1} bw per day of MnO_2-MPs, no statistically significant damage was observed after a 28-day repeated oral dose treatment in comparison to the control ($P > 0.05$). In the present study, an i.p. injection of CP (40 mg kg^{-1} bw) induced DNA damage in rat peripheral blood leukocytes. The mean % tail DNA was significantly ($P < 0.01$) higher compared with the control.

Micronucleus Test

The bone marrow MNT was conducted after 28-day repeated oral treatment with 30, 300, 1000 mg kg^{-1} bw per day of MnO_2-NPs and MnO_2-MPs in male and female Wistar rats. The MNT data indicated statistically significant enhancement in MN-PCEs frequency in the MnO_2-NPs treated groups with higher and medium doses (1000, 300 mg kg^{-1} bw per day) in rats (Fig. 2B). However, the dose of 30 mg kg^{-1} bw per day was not significant ($P > 0.05$). The MnO_2-MPs-treated groups showed a significant increase in the frequency of MN-PCEs only with the higher dose (1000 mg/kgbw/day) group of animals. On the other hand, the CP (40 mg kg^{-1} bw)-treated group induced a substantially significant ($P < 0.01$) effect on MN-PCEs frequency. The various doses of MnO_2-NPs and MnO_2-MPs exhibited an insignificant decrease in % PCEs in comparison to the negative control in both male and female rats in the MNT (Fig. 2C).

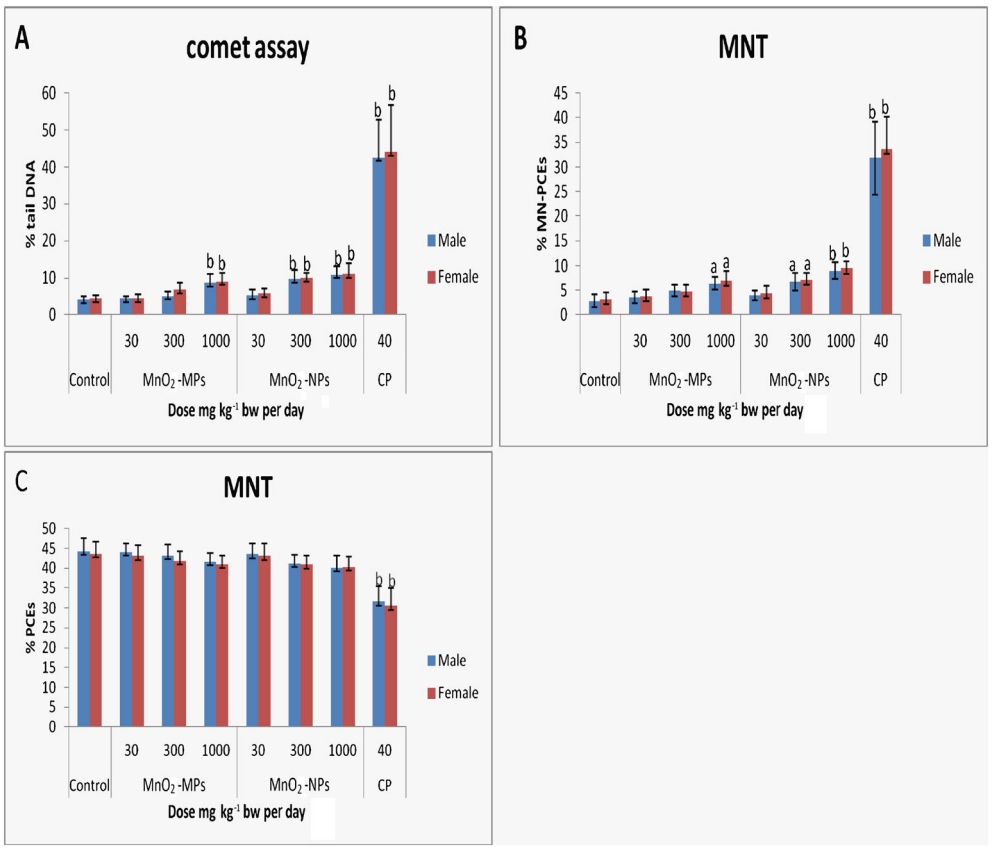

Figure 2. The *in vivo* genotoxicity of manganese oxide nanoparticles (MnO_2-NPs) and MnO_2-microparticles (MPs). (A) Mean % tail DNA in peripheral blood leucocytes of male and female Wistar rats observed after 28-day repeated oral doses of MnO_2-NPs and MnO_2-MPs, (B) Frequency of MN-PCEs in male and female Wistar rat bone marrow cells conducted after 28-day repeated oral doses of MnO_2-NPs and MnO_2-MPs, (C) Percentage PCEs in male and female Wistar rat bone marrow cells conducted after 28-day repeated oral doses of MnO2-NPs and MnO2-MPs. Deionised water (control), CP (cyclophosphamide, positive control), Data represented as mean±SD. Significantly different from control at Significantly different from control at a = < 0.05, b = $P < 0.01$, $n = 5$ animals per group.

Chromosomal Aberration Assay

The results of the chromosomal aberration assay determined after the oral administration of MnO_2-NPs and MnO_2-MPs for 28 days at various doses (30, 300 and 1000 mg kg^{-1} bw per day) to Wistar male and female rats in bone marrow cells are shown in Table 2, 3. The MnO_2-NPs induced significant CAs at 1000 and 300 mg kg^{-1} bw per day dose levels. In addition, the NPs at 1000 and 300 mg kg^{-1} bw per day revealed the same significant increase in structural and numerical CA as well as percentage of abnormal cells in rats. However, MnO_2-NPs did not show a significant increase ($P > 0.05$) of CA with the 30 mg kg^{-1} bw per day dose. Further, MnO_2-MPs caused a significant increase ($P > 0.01$) in the total cytogenetic changes, structural (gaps, breaks, minute, acentric fragment and reciprocal translocation), numerical (aneuploidy) CAs and percentage (%) of aberrant cells at 1000 mg kg^{-1} bw per day in all the animals (Table 2,3). The MI was used to conclude the rate of cell division. MnO_2-NPs and MnO_2-MPs at the higher dose (1000 mg/kgbw/day) exposure did not significantly decrease the MI. MnO_2-NPs and MnO_2-MPs did not reveal any differences in MI after the medium and low dose of 300 and 30 mg kg^{-1} bw per day as compared with the control groups (Table 2,3).

Biochemical Enzyme Alterations

The 28-day repeated oral treatment of rats with MnO_2-NPs revealed that RBC and brain AChE were inhibited in a dose-dependent manner compared with controls in both male and female rats. There was significant ($P < 0.01$) inhibition in the RBC AChE level at 300 and 1000 mg kg^{-1} bw per day dose of the MnO_2-NPs-treated groups and significant ($P < 0.05$) changes at 1000 mg kg^{-1} bw per day dose when treated with MnO_2-MPs as compared with the control in both male and female rats (Fig. 3A and 4A). In the brain, MnO_2-NPs induced significant ($P < 0.01$) inhibition at all three doses 30, 300 and 1000 mg kg^{-1} bw per day in both male and females as compared with the control. However, MnO_2-MPs induced a significant ($P < 0.05$) inhibition in brain AChE only at 1000 mg kg^{-1} bw per day (Fig. 3B and 4B).

Total, Na^+-K^+, Mg^{2+} and Ca^{2+}-ATPases were significantly ($P < 0.01$) inhibited at all the three doses of MnO_2-NPs in the brain of male and female rats. In addition, the changes observed were dose dependent. Similarly, both male and female rats exposed to 300 and 1000 mg kg^{-1} bw doses of MnO_2-MPs showed a significant decline in the total ATPases and Mg^{2+}-ATPases. Further, a significant ($P < 0.05$) decline in Na^+-K^+ and Ca^{2+}-ATPases was found in rats exposed to 1000 mg kg^{-1} bw dose of MnO_2-MPs (Fig. 3C and 4C).

The repeated doses of MnO_2-NPs significantly increased the AST activity in the liver and serum but it was decreased in kidney in a dose-dependent manner. Moreover, as the dose increased, the ALT activity also increased in serum, the liver and kidney after repeated treatment with MnO_2-NPs in male and female rats (Figs 3D–F and 4D–F). The AST activity increased significantly in serum at 300 and 1000 mg kg^{-1} bw per day ($P < 0.01$) doses in rats. Serum ALT, liver AST and ALT increased significantly at all doses in male and female rats. Further, kidney AST decreased significantly at all the three doses whereas the kidney ALT level increased at the 1000 mg kg^{-1} bw dose only. The alterations observed by the treatment of MnO_2-MPs were mostly insignificant with few exceptions. The changes in serum ALT, liver and kidney AST level at higher doses were observed to be significant.

The repeated doses of MnO_2-NPs showed an increase in serum, liver and kidney LDH activity in a dose-dependent manner in both male and female rats (data not shown). The serum LDH significantly increased ($P < 0.01$) at all the doses. However, the liver and kidney LDH level was significantly ($P < 0.05$ and $P < 0.01$) activated at 300 and 1000 mg kg^{-1} bw per day doses, respectively. Owing to the treatment of MnO_2-MPs, the LDH activity in serum showed a significant increase at 1000 mg kg^{-1} bw per day dose in rats ($P < 0.01$) (data not shown).

Histopathological Examinations

Significant tissue damage was observed in the tissues obtained from rats treated with 1000 mg kg^{-1} bw per day dose of MnO_2-NPs. The photomicrograph of liver tissue showed an expanded portal tract with periportal inflammation (Fig. 5B). Hepatic fibrosis and hydropic degeneration was also seen. The histopathological picture of the kidney is shown in Fig. 5E. Necrosis and swelling of the proximal tubule was observed. Focal tubular damage and swelling in the renal glomerulous was also found. Spleen lesions and splenic hyperplasia associated with exposure to MnO_2-NPs in high dose groups was found. Congested red and white pulp of the spleen is shown in Fig. 5I. Inflammation in spleen tissues was observed. Many neurotropic cells were also found. The rats had brain inflammation owing to exposure to MnO_2-NPs. Vacuoles were also observed in the neurons (Fig. 5G). However, there were no abnormal pathological changes in the heart and lungs of the nanoform of the MnO_2-treated groups (data not shown). Hydropic degeneration, dilation around the central vein and scattered hepatocytic necrosis was observed in the rats of the 1000 mg kg^{-1} bw per day group treated with MnO_2-MPs (Fig. 5C). No other significant histopathological changes were found in the heart, lungs, kidney, brain, spleen of 1000 mg kg^{-1} bw per day MnO_2-MPs treated rats (data not shown). Further, there were no evident effects in the low- and medium-dose groups of nano- and micro-sized MnO_2.

Mn content analysis

Repeated exposure of MnO_2-NPs and MnO_2-MPs for 28 days with various doses 30, 300 and 1000 mg kg^{-1} bw per day in male and female Wistar rats was found to result in a significant increase in Mn concentration, indicating that absorption of Mn had occurred (Fig. 6). Mn accumulated significantly in all the tissues i.e. whole blood, the liver, heart, kidneys and spleen in the groups of animals treated with MnO_2-NPs and MnO_2-MPs. The maximum amount of Mn was distributed in the liver, kidney, spleen and blood. The distribution of Mn was maximum in 1000 mg kg^{-1} bw per day followed by 300 and 30 mg kg^{-1} bw per day of male and female rats treated with MnO_2-NPs and MnO_2-MPs. However, the absorption of Mn in various tissues was very high in the NPs-treated groups as compared to MPs-treated groups at all dose levels. In the MnO_2-NPs-treated rats, a significant amount of Mn was removed via urine. The maximum excretion of Mn was found with 1000 mg kg^{-1} bw followed by 300 and 30 mg kg^{-1} bw. In contrast, MnO_2-MPs-treated rats showed large excretion in feces.

Discussion

In the near future, nanotechnology will play an important part in the world's economy and in our everyday lives. In spite of the

Table 2. Chromosome aberrations and percent mitotic index observed in bone marrow cells of female Wistar rats after 28-day repeated oral treatment with manganese oxide nanoparticles (MnO_2-NPs) and MnO_2-microparticles (MPs)

Dose (mg/kg b.w.)	M.I. (%)	Chromosomal aberrations							Aberrant cells (%)	Total cytogenetic changes	TA + gaps M±SE	TA-gaps M±SE
		Numerical aberrations		Structural aberrations								
		Aneuploidy	Polyploidy	Gaps	Breaks	Minute	Acentric Fragments	Reciprocal translocations				
Con.[a]	3.41±0.40	1.2±0.8	0.0±0.0	1±1	0.4±0.5	0.2±0.4	0.4±0.5	0.00±00	0.6±0.51	3.2±1.6	2.0±0.9	1.0±0.6
MnO_2-NPs 30	3.30±0.59	2.0±0.7	0.0±0.0	2.0±0.7	1.4±0.5	1±0.7	1.4±1.1	0.0±00	3.1±1.02	7.8±1.9	5.8±1.6	3.8±0.9
300	3.27±0.47	4.6±2.0	0.0±0.0	3.8±1.9	3.2±1.7	2.0±0.7	2.6±1.5	0.0±00	6.0 ±1.5[b]	16.2±5.8[b]	11.6±2.9[b]	7.8±1.8[b]
1000	3.18±0.53	7.6±1.6	0.0±0.0	6.2±2.9	4.0±2.0	2.8±1.4	3.0±1.8	0.0±00	10.1±1.13[b]	23.6±6.9[b]	16.0±4.2[b]	9.8±2.3[b]
MnO_2-MPs 30	3.33±0.24	1.6±1.1	0.0±0.0	1.2±0.8	0.4±0.5	0.4±0.5	0.4±0.5	0.0±0.0	1.7±0.9	4.0±1.5	2.4±1.1	1.2±0.7
300	3.30±0.57	2.6±0.8	0.0±0.0	1.6±1.1	1.0±0.7	1.0±1	1.2±1.0	0.0±0.0	2.4±1.07	7.4±1.8	4.6±1.5	3.2±1.6
1000	3.20±0.59	4.4±2.0	0.0±0.0	4.4±1.5	2.6±1	1.8±1.2	3.0±0.8	0.0±0.0	6.0±1.5[b]	16.2±3.7[b]	11.8±2.7[b]	7.4±2.5[b]
CP[b]	1.88±0.63	36.8±4.9[b]	4.0±1[b]	12.4±3.4[b]	9.8±1.9[b]	12.8±3.0[b]	12.4±1.6[b]	2.4±1.6 [b]	38.5±2.7[b]	90.6±10.9[b]	49.8±8.3[b]	37.4±8.5[b]

Significantly different from control at a = $P < 0.05$, b = $P < 0.01$. One hundred metaphases were analyzed per animal; n = five animals per group.
Total cytogenetic changes = numerical aberrations and structural aberrations. % aberrant cells correspond to cells with ≥ 1 aberration excluding gaps. MI, mitotic index; data represented as mean±standard deviation; TA, total aberrations = structural aberrations.
[a]Negative control – deionized water.
[b]Cyclophosphamide (40 mg kg^{-1}).

Journal of Applied Toxicology

Table 3. Chromosome aberrations and percent mitotic index observed in bone marrow cells of male Wistar rats after a 28-day repeated oral treatment with manganese oxide nanoparticles (MnO_2-NPs) and MnO_2-microparticles (MPs)

Dose (mg/kg b.w.)	M.I. (%)	Chromosomal aberrations							Aberrant cells (%)	Total cytogenetic changes	TA + gaps M±SE	TA-gaps M±SE
		Numerical aberrations		Structural aberrations								
		Aneuploidy	Polyploidy	Gaps	Breaks	Minute	Acentric Fragments	Reciprocal translocations				
Con.[a]	3.38±0.54	1.6±1.1	0.0±0.0	1.4±0.8	0.6±0.5	0.8±0.8	0.4±0.5	0.00±00	1.1±0.7	2.6±1.5	3.2±0.7	1.8±0.9
MnO_2-NPs 30	3.18±0.30	2.4±0.5	0.0±0.0	3.0±1.5	1.2±1	1.6±0.9	1.6±0.8	0.00±00	2.4±1.4	9.8±2.3	7.4±0.9	4.4±1.3
300	2.98 ±0.24	4.4 ±1.9	0.0 ±0.0	4.8 ±1.7	3.0 ±1.8	2.2 ±1	3.0 ±1.5	0.00 ±00	5.1 ±2.1[b]	17.4 ±4.3[b]	13 ±2.3[b]	8.2 ±2.4[b]
1000	2.96 ±0.43	8.2 ±2.3	0.0 ±0.0	7.4 ±2.5	3.8 ±2.1	3 ±1.2	4.2 ±1.7	0.00 ±00	9.3 ±2.7[b]	26.6 ±4.7[b]	18.4 ±4.7[b]	11 ±3.9[b]
MnO_2-MPs 30	3.30 ±0.42	2.0 ±1	0.0 ±0.0	1.8 ±1.2	1.2 ±1	1.0 ±0.9	0.8 ±0.4	0.0 ±0.0	0.9 ±0.8	6.8 ±2.7	4.8 ±1.6	3.0 ±1.0
500	3.23 ±0.46	3.6 ±1.3	0.0 ±0.0	2.0 ±0.7	1.8 ±1.3	1.4 ±0.8	1.8 ±0.4	0.0 ±0.0	2.0 ±1.2	10.6 ±3.2	7.0 ±2.5	5.0 ±1.6
1000	3.03 ±0.36	4.6 ±2.0	0.0 ±0.0	2.8 ±.9	2.2 ±1.3	1.8 ±0.8	2.2 ±0.9	0.0 ±0.0	5.0 ±2.2[b]	13.6 ±2.3[b]	9.0 ±2.6[b]	6.2 ±2.8[b]
CP[b]	1.80 ±0.49	37.2 ±5.2[b]	4.6 ±1.3[b]	14.2 ±3.1[b]	11.4 ±2.3 [b]	13.4 ±3.2[b]	14.4 ±2.9[b]	2.4 ±1.1[b]	37.3 ±3.5[b]	97.6 ±10[b]	55.8 ±9.3[b]	41.6 ±3.9[b]

Significantly different from control at a = $P < 0.05$, b = $P < 0.01$. One hundred metaphases were analyzed per animal; n = five animals per group.
Total cytogenetic changes = numerical aberrations and structural aberrations.% aberrant cells correspond to cells with ≥ 1 aberration excluding gaps. MI, mitotic index; data represented as mean±standard deviation; TA, total aberrations = structural aberrations.
[a]Negative control – deionized water.
[b]Cyclophosphamide (40 mg kg^{-1}).

Journal of Applied Toxicology

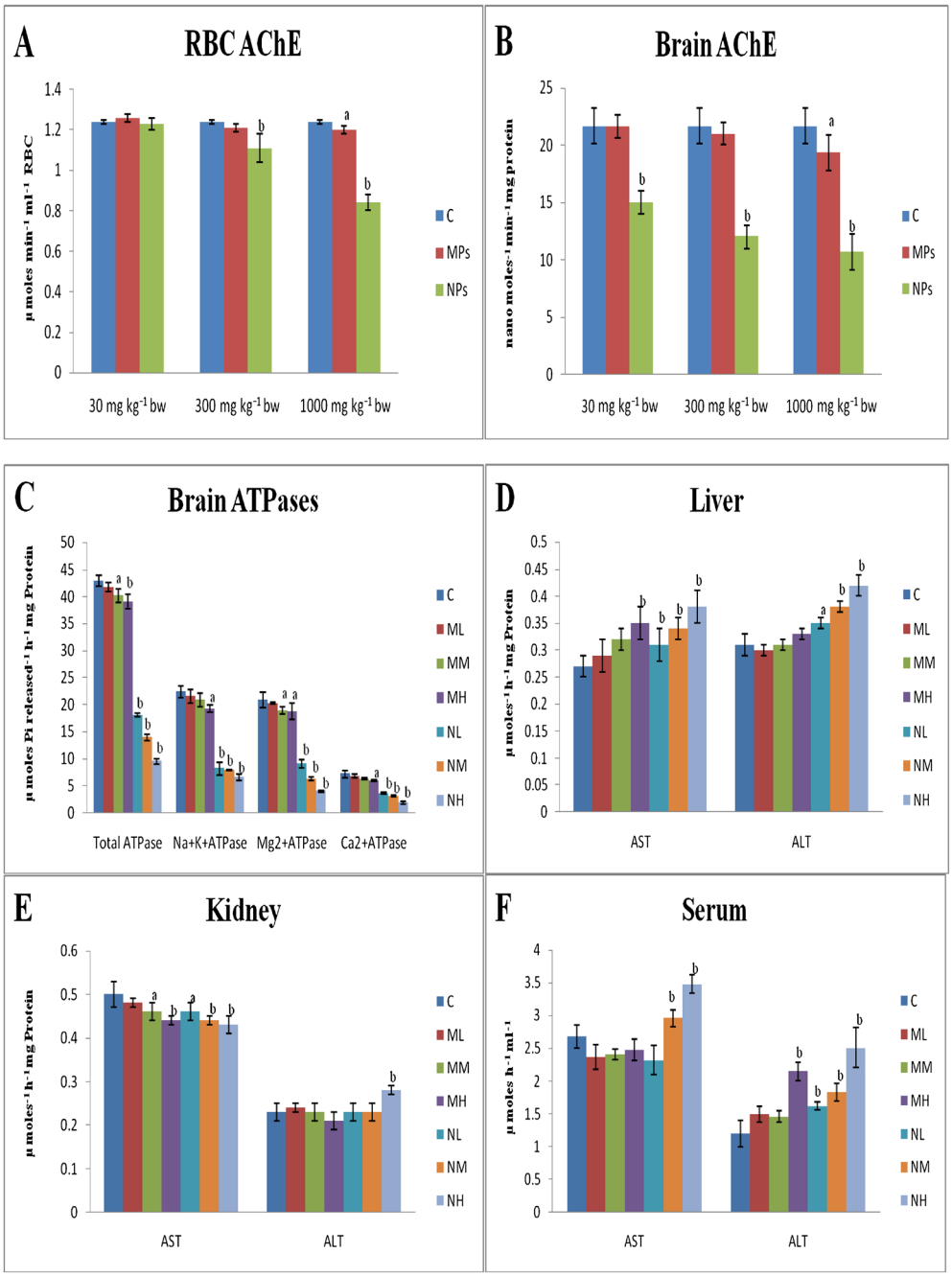

Figure 3. Biochemical changes in male rats. (A) Red blood cell (RBC) acetylcholinesterase (AChE), (B) brain AChE, (C) different brain ATPases, (D) liver aspartate minotransferase (AST) and liver alanine aminotransferase (ALT), (E) kidney AST and kidney ALT, (F) serum AST and serum ALT. ML = 30 mg kg^{-1} bw per day of MnO_2-MPs, MM = 300 mg kg^{-1} bw per day of MnO_2-MPs, MH = 1000 mg kg^{-1} bw per day of MnO_2-MPs, NL = 30 mg kg^{-1} bw per day of MnO_2-NPs, NM = 300 mg kg^{-1} bw per day of MnO_2-NPs, NH = 1000 mg kg^{-1} bw per day MnO_2-NPs, a = < 0.05, b = $P < 0.01$.

great prospects of nanotechnology, there are increasing worries that intentional or accidental human and environmental exposure to NPs may lead to significant toxic effects. The small size of NPs and their large surface area enables them to enter the human body via different routes. Hence, they represent a new cause of concern to humans and the environment possibly because of the increasing use of NPs even although their toxicity remains largely unexplored. The present study will provide the first evidence of the genotoxic, biochemical and biodistribution of the Mn in different tissues, urine and feces with MnO_2-NPs and MnO_2-MPs in albino Wistar male and female rats after 28 days of repeated oral treatment. The results of the present study revealed that MnO_2-NPs and MnO_2-MPs induced toxic effects but not death or severe suffering with a higher dose (1000 mg kg^{-1} bw per day). The test compounds in this study can be categorized as substances with toxic effects when taken for a long period of time.

The results obtained by the comet assay showed that MnO_2-NPs were able to cause the significant % tail DNA in peripheral blood leucocytes at a higher and medium dose as compared with the control. However, MnO_2-MPs revealed a significant increase in % tail DNA only at 1000 mg kg^{-1} bw per day in both

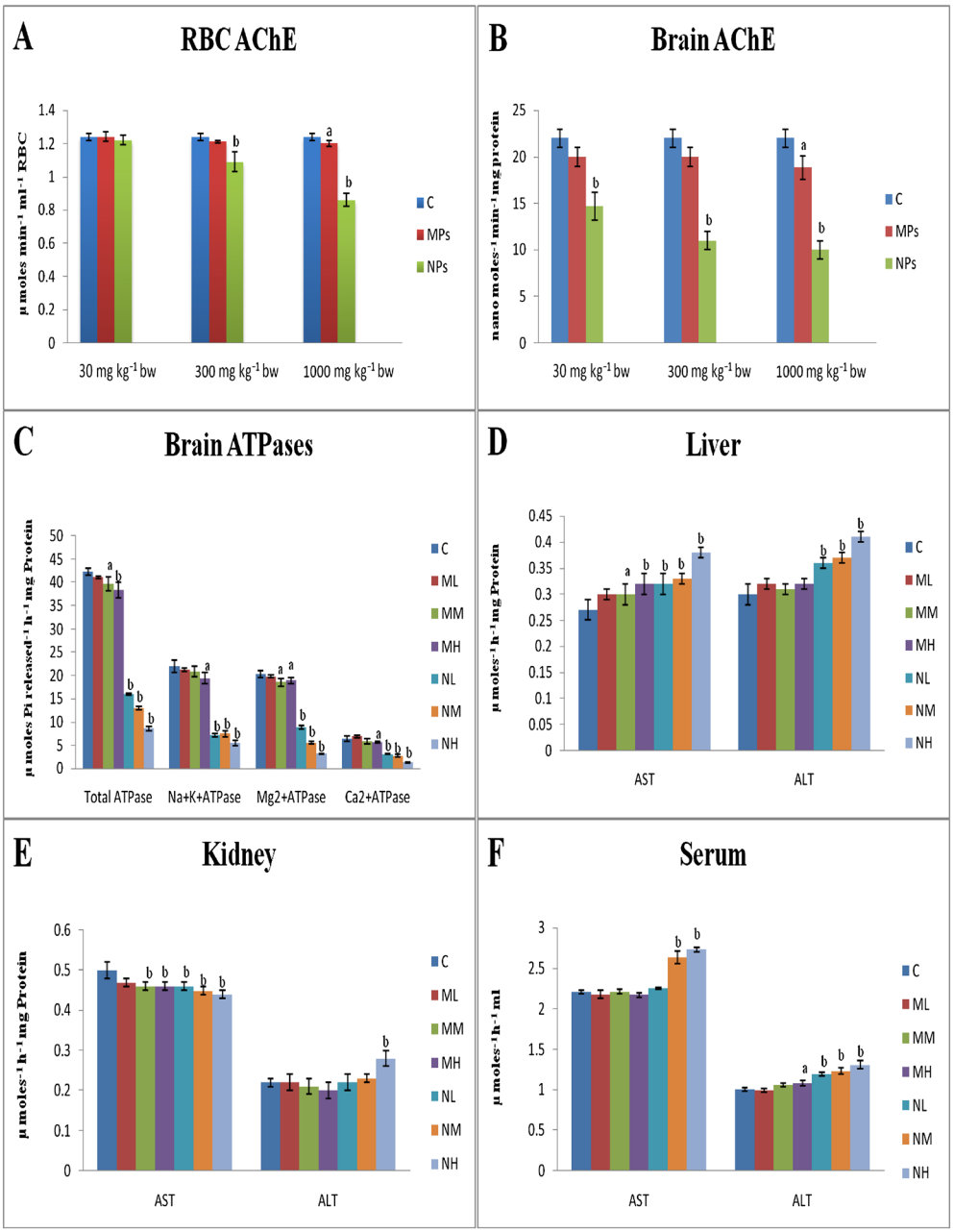

Figure 4. Biochemical changes in female rats. (A) Red blood cell (RBC) acetylcholinesterase (AChE), (B) brain AChE, (C) different brain ATPases, (D) liver aspartate minotransferase (AST) and liver alanine aminotransferase (ALT), (E) kidney AST and kidney ALT, (F) serum AST and serum ALT. ML = 30 mg kg^{-1} bw per day of MnO_2-MPs, MM = 300 mg kg^{-1} bw per day of MnO_2-MPs, MH = 1000 mg kg^{-1} bw per day of MnO_2-MPs, NL = 30 mg kg^{-1} bw per day of MnO_2-NPs, NM = 300 mg kg^{-1} bw per day of MnO_2-NPs, NH = 1000 mg kg^{-1} bw per day MnO_2-NPs, a = < 0.05, b = $P < 0.01$.

male and female rats. Some previous studies are in agreement with our findings. For example, when $MnCl_2$ was given in drinking water to male Wistar rats for 30 days consecutively, significant DNA damage and ROS production in the liver was observed (Chtourou *et al*., 2013). Likewise, $MnCl_2$ injected i.p. in rats at 5, 10, and 20 mg kg^{-1} bw daily for 3 months, showed a significant increase in mitochondrial DNA damage in rat brain and the liver (Jiao *et al*., 2008). Similarly, when mice were given ZnO-NPs by the oral route for 14 continuous days, a significant increase in DNA damage with the comet assay in the liver at the higher dose was found (Sharma *et al*., 2012). TiO_2-NPs administered in drinking water for 5 days induced DNA damage in blood leukocytes with the comet assay in mice (Trouiller *et al*., 2009).

The bone marrow MNT results revealed a significant increase in the MN frequency at 1000 mg kg^{-1} bw per day and 300 mg kg^{-1} bw per day as compared with the control, suggesting genotoxicity of MnO_2-NPs. Further, MNT indicated that rats exposed to 1000 mg kg^{-1} bw per day of MnO_2-MPs were significant in both genders. The % PCEs calculated in the MnO_2-NPs and MnO_2-MPs treated groups induced a slight decrease compared with the control group suggesting that cell death had occurred in the treated groups. It is possible that clastogenic events are involved in the formation of these MN with MnO_2-NPs and MnO_2-MPs. Our findings are in concurrence with a study in mice which demonstrated a significant increase in the MN frequency in PCEs, when TiO_2-NPs

Journal of AppliedToxicology

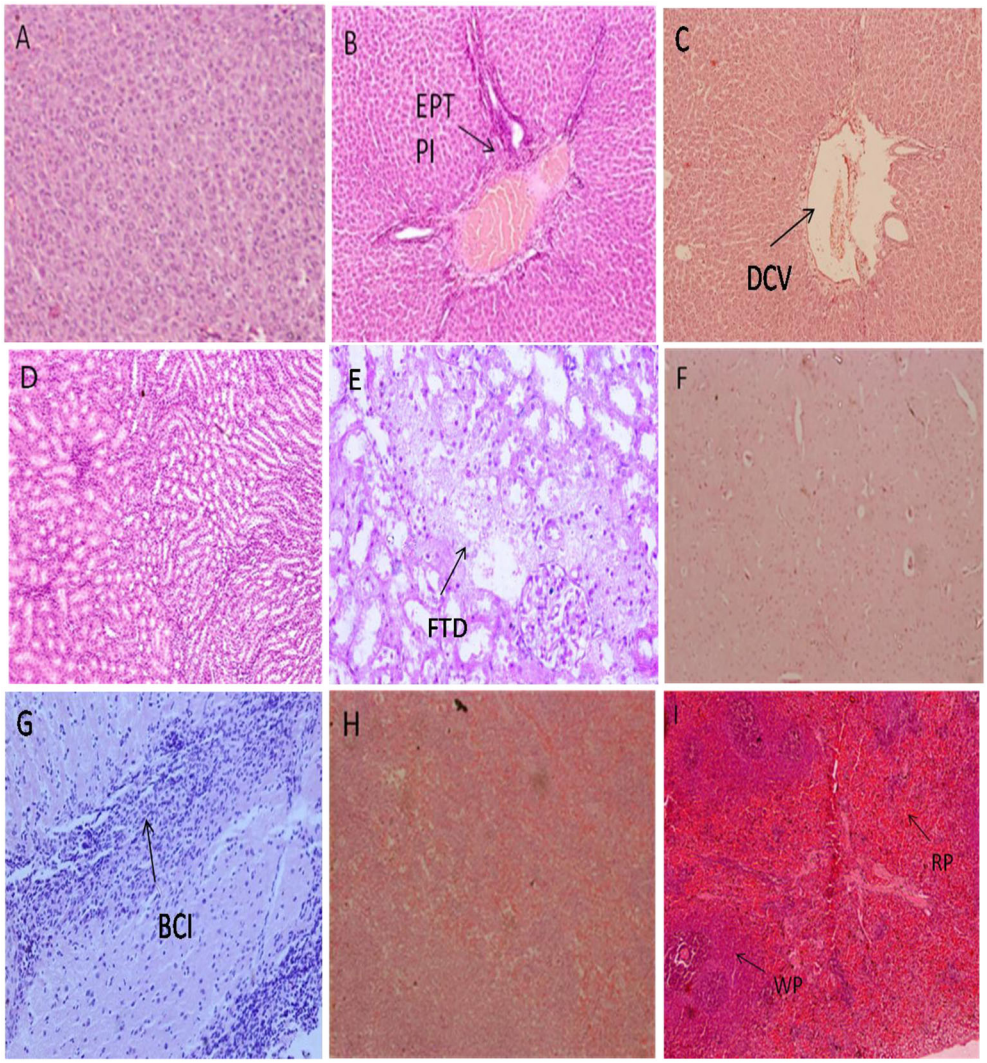

Figure 5. Photomicrograph of the liver, kidney, brain and spleen. Normal architecture of the liver (A), kidney (D), brain (F) and spleen (H). The manganese oxide nanoparticles (MnO_2-NPs) of treated rats at 1000 mg kg^{-1} bw per day after 28 days repeated dosing induced changes in the liver (B), kidney (E), brain (G) and spleen with splenic hyperplasia (I) and the MnO2-microparticles (MPs) at 1000 mg kg^{-1} bw showing changes in the liver (C). EPT, expanded portal tract; PI, periportal inflammation; DCV, dilated central vein; FTD, focal tubular damage; BCI, brain cell inflammation; RP, red pulp; WP, white pulp; (hematoxylin and eosin, 400×).

were administered in drinking water for 5 days (Trouiller *et al*., 2009).

The results of the CA analysis with MnO_2-NPs and MnO_2-MPs in rats indicated that MnO_2-NPs were able to induce significant cytogenetic changes with the 1000 and 300 mg kg^{-1} bw per day doses but not with 30 mg kg^{-1} bw per day. However, MnO_2-MPs induced significant CA in bone marrow cells only at 1000 mg kg^{-1} bw per day. The MI results suggested a decrease in its values as compared with the control groups. This could be as a result of a slower progression of cells from the S (DNA synthesis) phase to the M (mitosis) phase of the cell cycle as a result of MnO_2-NPs and MnO_2-MPs exposure, although it is most likely that this impairment in cell cycle progression is associated with MnO_2-NPs and MnO_2-MPs toxicity. The mechanisms responsible for the genotoxicity of NPs involve oxidative stress which cause redox imbalance with in cells usually as a result of an increase in intracellular ROS. Generated ROS in the metabolizing cells could attack DNA base guanine and form 8-OHdG lesions, which are known to have a mutagenic potential (Singh *et al*., 2009). An *in vitro* study in which PC-12 cells were exposed to MnO_2 NPs showed a >10-fold ROS generation and significant dopamine depletion in a dose-dependent manner (Hussain *et al*., 2006). Similarly, when rat type II alveolar epithelial cells were exposed to Mn_3O_4-NPs, they revealed a significant increase in the ROS generation and dose-dependent increase in apoptotic cells by the TUNEL assay (Frick *et al*., 2011). Likewise, when $MnCl_2$ was injected i.p. at 15 and 30 mg kg^{-1} bw per day to rats, significant ROS was generated in the liver and brain mitochondria (Zhang *et al*., 2003). Our 28-day repeated oral toxicity study revealed genotoxic effects with the MnO_2-NPs and MnO_2-MPs in albino Wistar male and female rats during the comet, MNT and CA assay. This might be as a resultof increased ROS. Mn^{2+} can generate both hydroxyl ($^{\cdot}OH$) and super-oxide ($^{\cdot}O_2^-$) radicals from H_2O_2 through the following equation: $Mn^{2+}+O_2 = Mn^{3+}+O_2^-$ and $Mn^{2+}+H_2O_2 = Mn^{3+}+OH^- + {}^{\cdot}OH$. The $^{\cdot}OH$ and $^{\cdot}O_2^-$ radicals can attack DNA bases and ribose to form base adducts, such as 8-OHdG, or abstract hydrogen from C1 or C4 of ribose, which results in single-strand breaks (Gerber *et al*., 2002).

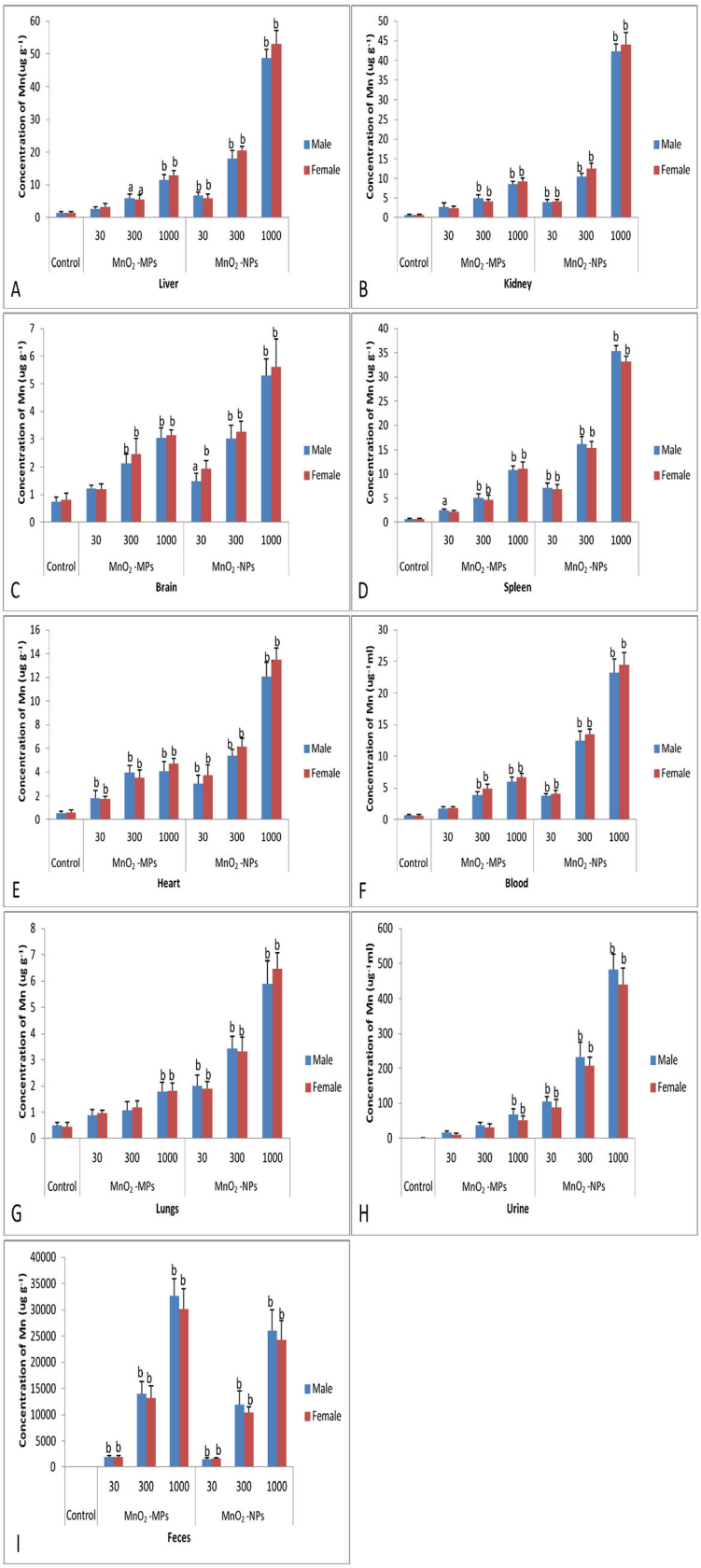

Figure 6. Tissue distribution of manganese (Mn) measured by inductively coupled plasma-mass spectrophometery (ICP-MS) in male and female Wistar rats after 28-day repeated oral doses of manganese oxide nanoparticles (MnO_2-NPs) and MnO2-microparticles (MPs)in the liver (A), kidney (B), brain (C), spleen (D), heart (E), blood (F), lungs (G), urine (H) and feces (I), a = < 0.05, b = $P < 0.01$.

In the present study, 28 day repeated MnO_2-NPs exposure significantly inhibited RBC and brain AChE in a dose-dependent manner in both male and female rats. Similarly, in a previous study, rats were administered with four or eight i.p. injections of 25 mg kg^{-1} bw of $MnCl_2$ on alternate days. The animals showed a significant decrease in brain AChE activity 24 h after the last injection (Santos *et al*., 2012). Activities of Total, Na^+-K^+, Mg^{2+} and Ca^{2+}-ATPases were significantly inhibited in a dose-dependent order in the brain of male and female rats owing to the exposure of MnO_2-NPs, indicating that nerve conduction might have been affected by NPs. Further, higher doses of MnO_2-MPs also showed inhibition of ATPase in rats. Similar inhibition of ATPase was found with other NPs. Hu *et al*. (2010) demonstrated significant inhibition of Na^+-K^+ and Ca^{2+}-ATPase in ICR mice. Huang *et al*. (2011) observed a significant decrease in the activities of Na^+-K^+, Mg^{2+} and Ca^{2+}-ATPases in hepatocyte mitochondria after 30 days of i.p. exposure of $MnCl_2$ in male Sprague–Dawley rats. It has been demonstrated that Na^+-K^+-ATPase have a significant role in the nervous system and involvement in neurologic diseases (Benarroch, 2011). Mn is broadly reported to be neurotoxic in the nano and bulk form both *in vitro* and *in vivo* (Stefanescu *et al*., 2009; Schroeter *et al*., 2012; Oszlanczi *et al*., 2010a). Our study showed that MnO_2-NPs caused significant alterations in activity of AST and ALT in serum, the liver and kidney of the exposed rats in a dose-dependent manner. MnO_2-MPs also induced changes in the liver and kidney AST and serum ALT in both sexes of rats. Likewise, sub-acute oral exposure of ZnO-NPs (300 mg kg^{-1} bw) for 14 consecutive days in mice elevated serum ALT level (Sharma *et al*., 2012).

The induction of the LDH level in serum, the liver and kidney owing to MnO_2-NPs exposure in dose-dependent manner in rats revealed that there may be injuries in tissues in contrast to the MnO_2-MPs and the control. Similarly, oral administration of $MnCl_2$ (20 mg ml^{-1}) for 30 days increased the activities of hepatotoxicity biomarkers such as AST, ALT and LDH levels when compared with the control in male Wistar rats (Chtourou *et al*., 2013). It is reported that NPs interact with proteins and enzymes and interfere with the antioxidant defense mechanism, leading to ROS generation causing apoptosis and necrosis (Schrand *et al*., 2010). Histomicrographs of rats treated with 1000 mg kg^{-1} bw per day dose of the nano form of MnO_2 showed changes in the liver, spleen, kidney and brain tissues. Similar alterations were observed with other metal NPs (Chen *et al*., 2009; Lei *et al*., 2008; Li *et al*., 2012; Wang *et al*., 2007).

The transportation of NPs from circulating blood to the tissues and binding to its molecular target could be a first step in NPs retention or cellular internalization. Numerous NPs are rapidly cleared from the blood stream by the reticulo-endothelial system (RES) and the mononuclear phagocytic system (MPS) mainly through the liver, spleen and bone marrow (Ferrari, 2005; Peer *et al*., 2007). The *in vivo* metabolic processes of MnO_2 NPs within the organism, as well as their distribution in the important tissues, are not yet completely understood.

Our biodistribution study revealed that MnO_2-NPs can pass across the gastrointestinal barrier and accumulate in the organs and tissues. The NPs were significantly distributed in the liver, spleen, kidney, heart, blood, brain and lungs. The majority of NPs were found in the liver, kidney as well as spleen. The excretion data showed that a little quantity of NPs was excreted via urine, whereas large amount of the NPs was excreted via feces. The tissue distribution of Mn with MnO_2-MPs-treated rats also showed a significant increase in the kidney, heart, spleen, lungs and blood with a high and medium dose and a little amount was observed with a low dose. The incorporation of Mn in the various tissues of the MnO_2-NPs-treated groups was in the range of 1.35–12.79% and it was 0.68–4.63% in the MP-treated groups. The excretion of the MnO_2-MPs was greater in feces in contrast to MnO_2-NPs. The excretion of MnO_2-NPs and MnO_2-MPs via urine was 0.72–1.6% and 0.11–0.93% (μg ml^{-1}), respectively, and 17.19–25.62% (μg g^{-1}) of the MnO_2-MPs and 14.44–23.51% (μg g^{-1}) of MnO_2-NPs was detected in the feces without any significant gender difference. The distribution pattern was dose dependent, as the amount absorbed increased as the dose administered increased. MnO_2-NPs showed a much higher absorption and tissue distribution as compared with MnO_2-MPs. Nonetheless a significant gender-related difference in the biodistribution of Mn was not found in the different tissues of male and female Wistar rats during 28 days of the repeated oral dose study. The Mn quantity was higher in the brain with the MnO_2-NPs-treated groups in comparison to MPs as well as control groups. Our study indicated that Mn can penetrate the blood–brain barrier (BBB). Many investigations have revealed that the divalent metal transporter-1 (DMT1) may be engaged in Mn influx into brain (Conrad *et al*., 2000). Mn binds to plasma transferrin (Tf). Hence, it has been suggested that transport of the Mn–Tf complex into the brain relies on a transferrin receptor (TfR)-dependent mechanism, which competes with Fe transport, or vice versa. However, recent investigations have shown that the lack of functional DMT1 in knock-out rats had no apparent effect on brain influx of Mn ion or Mn-Tf (Crossgrove and Yokel, 2004).

Some previous studies with MnO_2-NPs but using different routes of administration such as intranasal instillation and intratracheal instillation are also in accordance with our findings (Elder et al., 2006; Oszlanczi *et al*., 2010b; Sárközi *et al*., 2009). Human and environmental exposure with MnO_2-NPs and MnO_2-MPs may be for a long duration. Hence, to gain insight in to genotoxicity, biochemical alterations and deposition of Mn particles including retention and possible distribution in the body, this study was initiated.

Conclusions

It is clear from our results that MnO_2-NPs produced toxicity at lower doses as compared with MnO_2-MPs with genotoxicity, biochemical, histopathology and biodistribution parameters. Further the NPs showed more bioaccumulation as compared with the MPs at the same dose level in male and female rats after 28 days of repeated oral dose study. The present results suggest that MnO_2-NPs and MnO_2-MPs do not induce a gender-related significant difference in the biodistribution of Mn in rats. This study does not imply that MnO_2-NPs should not be used for biological or medical purposes. In our investigation high doses were used to get genotoxicity and biochemical changes of the NPs after absorption in to the rats.

Conflict of interest

There are no conflicts of interest.

Acknowledgements

This work was financially supported by Department of Biotechnology, New Delhi, India (Grant No. BT/PR9998/NNT/28/84/

2007). Further, Shailendra Pratap Singh (SRF) is grateful to Indian Council of Medical Research, India and Monika Kumari (SRF) is grateful to University Grant Commission, India for the award of fellowship.

References

Adler ID. 1984. Cytogenetic tests in mammals. In *Mutagenicity Testing: A Practical Approach* Venitt S, Parry J (eds). IRL Press: Oxford; 273–306.

Benarroch EE. 2011. Na^+, K^+ - ATPase: functions in the nervous system and involvement in neurologic disease. *Neurology* **76**: 287–293.

Chen H, He J. 2008. Facile synthesis of monodisperse manganese oxide nanostructures and their application in water treatment. *J. Phys. Chem. C* **112**: 17540–17545.

Chen J, Dong X, Zhao J, Tang G. 2009. In vivo acute toxicity of titanium dioxide nanoparticles to mice after intraperitioneal injection. *J. Appl. Toxicol.* **29**: 330–337.

Choi JY, Lee SH, Na HB, An K, Hyeon T, Seo TS. 2010. In vitro cytotoxicity screening of water-dispersible metal oxide nanoparticles in human cell lines. *Bioprocess Biosyst. Eng.* **33**: 21–30.

Chtourou Y, Garoui EM, Boudawara T, Zeghal N. 2013. Therapeutic efficacy of silymarin from milk thistle in reducing manganese induced hepatic damage and apoptosis in rats. *Hum. Exp. Toxicol.* **32**: 70–81.

Conrad ME, Umbreit JN, Moore EG, Hainsworth LN, Porubcin M, Simovich MJ, Nakada MT, Dolan K, Garrick MD. 2000. Separate pathways for cellular uptake of ferric and ferrous iron. *Am. J. Physiol. Gastrointest. Liver Physiol.* **279**: G767–G774.

Crossgrove JS, Yokel RA. 2004. Manganese distribution across the blood–brain barrier III. The divalent metal transporter-1 is not the major mechanism mediating brain manganese uptake. *Neurotoxicology* **25**: 451–460.

Elder A, Gelein R, Silva V, Feikert T, Opanashuk L, Carter J, Potter R, Maynard A, Ito Y, Finkelstein J, Oberdörster G. 2006. Translocation of inhaled ultrafine manganese oxide particles to the central nervous system. *Environ. Health Perspect.* **114**: 1172–1178.

Ellman GL, Courtney KD, Anders RJR, Featherstone RM. 1961. A new and rapid colometric determination of acetylcholinestrase activity. *Biochem. Pharmacol.* **7**: 88–95.

Ferrari M 2005. Cancer nanotechnology: opportunities and challenges. *Nat. Rev. Cancer* **5**: 161–171.

Fischer HC, Chan WCW. 2007. Nanotoxicity: the growing need for in vivo study. *Curr. Opinion Biotechnol.* **18**: 565–571.

Fiske CH, Subbarow Y. 1925. The Colorimetric Determination of Phosphorus. *J. Biol. Chem.* **66**: 375–400.

Frick R, Müller-Edenborn B, Schlicker A, Rothen-Rutishauser B, Raemy DO, Günther D, Hattendorf B, Stark W, Beck-Schimmer B. 2011. Comparison of manganese oxide nanoparticles and manganese sulfate with regard to oxidative stress, uptake and apoptosis in alveolar epithelial cells. *Toxicol. Lett.* **205**: 163–172.

Gerber GB, Leonard A, Hantson P. 2002. Carcinogenicity, mutagenicity and teratogenicity of manganese compounds. *Crit. Rev. Oncol. Hematol.* **42**: 25–34.

Hu R, Gong X, Duan Y, Li N, Che Y, Cui Y, Zhou M, Liu C, Wang H, Hong F. 2010. Neurotoxicological effects and impairment of spatial recognition memory in mice caused by exposure to TiO_2 nanoparticles. *Biomaterials* **31**: 8043–8050.

Huang P, Chen C, Wang H, Li G, Jing H, Han Y, Liu N, Xiao Y, Yu Q, Liu Y, Wang P, Shi Z, Sun Z. 2011. Manganese effects in the liver following subacute and subchronic manganese chloride exposure in rats. *Ecotoxicol. Environ. Saf.* **74**: 615–622.

Hussain SM, Hess KL, Gearhart JM, Geiss KT, Schlager JJ. 2005. In vitro toxicity of nanoparticles in BRL 3A rat liver cells. *Toxicol. In Vitro* **19**: 975–983.

Hussain SM, Javorina AK, Schrand AM, Duhart HM, Ali SF, Schlager JJ. 2006. The interaction of manganese nanoparticles with PC-12 cells induces dopamine depletion. *Toxicol. Sci.* **92**: 456–463.

Jiao J, Qi Y, Fu J, Zhou Z. 2008. Manganese-induced single strand breaks of mitochondrial DNA in vitro and in vivo. *Environ. Toxicol. Pharmacol.* **26**: 123–127.

Jinna RR, Uzodinma JE, Desaiah D. 1989. Age-related changes in rat brain ATPases during treatment with Chlordecone. *J. Toxicol. Env. Health* **27**: 199–208.

Lei R, Wu C, Yang B, Ma H, Shi C, Wang Q, Wang Q, Yuan Y, Liao M. 2008. Integrated metabolomic analysis of the nano-sized copper particle-induced hepatotoxicity and nephrotoxicity in rats: a rapid in vivo screening method for nanotoxicity. *Toxicol. Appl. Pharmacol.* **232**: 292–301.

Li CH, Shen CC, Cheng YW, Huang SH, Wu CC, Kao CC, Liao JW, Kang JJ. 2012. Organ biodistribution, clearance, and genotoxicity of orally administered zinc oxide nanoparticles in mice. *Nanotoxicology* **6**: 746–756.

Limbach LK, Wick P, Manser P, Grass RN, Bruinink A, Stark WJ. 2007. Exposure of engineered nanoparticles to human lung epithelial cells: influence of chemical composition and catalytic activity on oxidative stress. *Environ. Sci. Technol.* **41**: 4158–4163.

Lowry OH, Rosenbhroough NJ, Farr AL, Randall RJ. 1951. Protein measurement with foiln phenol reagent. *J. Biol. Chem.* **193**: 265–275.

McQueen MJ. 1972. Optimal assay of LDH and α-HBD at 37°C. *Ann. Clin. Biochem.* **9**: 21–25.

Murdock RC, Braydich-Stolle L, Schrand AM, Schlager JJ, Hussain SM. 2008. Characterization of nanomaterial dispersion in solution prior to *in vitro* exposure using dynamic light scattering technique. *Toxicol. Sci.* **101**: 239–253.

Na HB, Lee JH, An K, Park YI, Park M, Lee IS, Nam DH, Kim ST, Kim SH, Kim SW, Lim KH, Kim KS, Kim SO, Hyeon T. 2007. Development of a T1 contrast agent for magnetic resonance imaging using MnO nanoparticles. *Angew. Chem. Int. Ed.* **46**: 5397–5401.

Nagwa HA, Kanthasamy A, Gu Y, Fang N, Anantharam V, Kanthasamy AG. 2011. Manganese nanoparticle activates mitochondrial dependent apoptotic signaling and autophagy in dopaminergic neuronal cells. *Toxicol. Appl. Pharmacol.* **256**: 227–240.

Nel A, Xia T, Madler L, Li N. 2006. Toxic potential of materials at the nanolevel. *Science* **310**: 622–627.

OECD. 1997a. Guidelines for genetic toxicology: micronucleus test. Guidelines 474. Organization for Economic Cooperation and Development: Paris.

OECD. 1997b. Guidelines for genetic toxicology: in vivo mammalian bone marrow cytogenetic test-chromosome analysis. Guidelines 475. Organization for Economic Cooperation and Development: Paris.

Oszlanczi G, Vezer T, Sarkozi L, Horvath E, Szabo A, Horvath E, Konya Z, Papp A. 2010a. Metal deposition and functional neurotoxicity in rats after 3–6 weeks nasal exposure by two physicochemical forms of manganese. *Ecotoxicol. Environ. Saf.* **30**: 121–126.

Oszlanczi G, Vezer T, Sarkozi L, Horvath E, Konya Z, Papp A. 2010b. Functional neurotoxicity of Mn-containing nanoparticles in rats. *Ecotoxicol. Environ. Saf.* **73**: 2004–2009.

Peer D, Karp JM, Hong S, Farokhzad OC, Margalit R, Langer R. 2007. Nanocarriers as an emerging platform for cancer therapy. *Nat. Nanotechnol.* **2**: 751–760.

Pool-Zobel BL, Lotzmann N, Knoll M, Kuchenmeister F, Lambertz R, Leucht U, Schröder HG, Schmezer P. 1994. Detection of genotoxic effects in human gastric and nasal mucosa cells isolated from biopsy samples. *Environ. Mol. Mutagen.* **24**: 23–45.

Rutz A. 2009. Synthesis and properties of manganese oxide nanoparticles for environmental applications. *The 2009 NNIN REU research accomplishments* 98–99.

Santos D, Milatovic D, Andrade V, Batoreu MC, Aschner M, dos Santos APM. 2012. The inhibitory effect of manganese on acetylcholinestrase activity enhances oxidative stress and neuro inflammation in the rat brain. *Toxicology* **292**: 90–98.

Sárközi L, Horvath E, Konya Z, Kiricsi I, Szalay B, Vezer T, Papp A. 2009. Subacute intratracheal exposure of rats to manganese nanoparticles: behavioral, electrophysiological, and general toxicological effects. *Inhal. Toxicol.* **21**: 83–91.

Schmid W 1975. The micronucleus test. *Mutat. Res.* **31**: 9–15.

Schrand AM, Rahman MF, Hussain SM, Schlager JJ, Smith DA, Ali SF. 2010. Metal based nanoparticles and their toxicity assessment. *Wiley Interdiscip. Rev. Nanomed. Nanobiotechnol.* **2**: 544–568.

Schroeter JD, Dorman DC, Yoon M, Nong A, Taylor MD, Andersen ME, Clewell III HJ. 2012. Application of multi-route physiologically based pharmacokinetic model for manganese to evaluate dose dependent neurological effects in monkeys. *Toxicol. Sci.* **129**: 432–446.

Service RF. 2005. Nanotechnology: call rise for more research on toxicology of nanomaterials. *Science* **310**: 1609.

Sharma V, Singh P, Pandey AK, Dhawan A. 2012. Induction of oxidative stress, DNA damage and apoptosis in mouse liver after sub-acute oral exposure to zinc oxide nanoparticles. *Mutat. Res.* **745**: 84–91.

Shin J, Rahman Md A, Ko MK, Im GH, Lee JH, Lee IS. 2009. Hollow manganese oxide nanoparticles as multifunctional agents for magnetic resonance imaging and drug delivery. *Angew. Chem. Int. Ed.* **48**: 321–324.

Singh N, Manshian B, Jenkins GJ, Griffiths SM, Williams PM, Maffeis TG, Wright CJ, Doak SH. 2009. NanoGenotoxicology: the DNA damaging potential of engineered nanomaterials. *Biomaterials* **30**: 3891–3914.

Stefanescu DM, Khoshnan A, Patterson PH, Hering JG. 2009. Neurotoxicity of manganese oxide nanomaterials. *J. Nanopart. Res.* **11**: 1957–1969.

Taira S, Kitajima K, Katayangi H, Ichiishi E, Ichiyanagi Y. 2009. Manganese oxide nanoparticle assisted laser desorption/ionization mass spectrometry for medical application. *Sci. Technol. Adv. Mater.* **10**: 1–6.

Tice RR, Agurell E, Anderson D, Burlinson B, Hartmann A, Kobayashi H, Miyamae Y, Rojas E, Ryu JC, Sasaki YF. 2000. The single cell gel/comet assay: Guidelines for in vitro and in vivo genetic toxicology testing. *Environ. Mol. Mutagen.* **35**: 206–221.

Trouiller B, Reliene R, Westbrook A, Solaimani P, Schiestl RH. 2009. Titanium dioxide nanoparticles induce DNA damage and genetic instability in vivo in mice. *Cancer Res.* **15**: 8784–8789.

Wang J, Zhou G, Chen C, Yu H, Wang T, Ma Y, Jia G, Gao Y, Li B, Sun J, Li Y, Jiao F, Zhao Y, Chai Z. 2007. Acute toxicity and biodistribution of different sized titanium dioxide particles in mice after oral administration. *Toxicol. Lett.* **168**: 176–185.

Yatzidis SH. 1960. Measurement of transaminases in serum. *Nature* **186**: 79–80.

Zhang S, Zhou Z, Fu J. 2003. Effect of manganese chloride exposure on liver and brain mitochondria function in rats. *Environ. Res.* **93**: 149–157.